

# EFFECTS OF THE LENGTH OF THE DAMAGE ZONE ON THE EFFECTIVE CONSTITUTIVE PROPERTIES OF AN ADHESIVE LAYER LOADED IN PEEL

Tobias Andersson and Anders Biel  
Department of Engineering Science, University of Skövde  
P.O. Box 408, SE-541 28 Skövde, Sweden  
[tobias.andersson@ite.his.se](mailto:tobias.andersson@ite.his.se) and [anders.biel@ite.his.se](mailto:anders.biel@ite.his.se)

## Abstract

An experimental method to determine the complete stress-elongation relation for a structural adhesive loaded in peel is presented. Experiments are performed on DCB specimens, which facilitate a stable experimental set-up. The method is based on the concept of equilibrium of the energetic forces acting on the specimen. By use of this concept, it is possible to measure the energy release rate as a function of the elongation of the adhesive layer instantaneously during an experiment. The complete stress-elongation relation is found to be the derivative of the energy release rate with respect to the elongation. To investigate whether or not the relation is a material property, experiments are performed on five different groups of specimens with different dimensions. This leads to large variations in the length of the damage zone heading a crack in the adhesive layer. It is found that the relation is independent of the geometry tested. Thus, the investigation supports that the stress-elongation relation can be considered as a material property.

## 1. Introduction

In recent years, the automobile industry has shown an increasing interest in adhesive joining. This depends on several factors. One is that the weight of the car has to be reduced in order to reduce the fuel consumption and emissions. To accomplish this, lightweight materials can be used. This puts demands on the joining method since mixed materials are likely to be a necessity. Adhesive joining appears to be a strong candidate in this respect. There is therefore a need for good material models and accurate data to be used in numerical simulations during the design process. However, these data are not easily obtained.

A substantial amount of work has considered linear-elastic fracture mechanics (LEFM) as a tool to predict fracture of adhesive joints. Several standards are based upon LEFM. By using LEFM, one disregards the actual fracture process taking place in the adhesive and assumes that the damage zone is much smaller than other relevant dimensions, *e.g.* the layer thickness. However, in reality the damage zone can be several layer-thicknesses long. The length of the damage zone depends on several factors *e.g.* the ductility of adhesive and the geometry of the specimen, *cf.* Andersson and Stigh [1].

A more attractive method is to make use of the adhesive layer theory. The method is attractive because it can be implemented into any finite element code. In the adhesive layer theory, the stresses and strains are assumed constant through the thickness of the adhesive layer. The behaviour of the layer is described with the peel (tension) stress,  $\sigma$ , the shear stress,  $\tau$ , the elongation,  $w$ , and the shear deformation,  $v$ , as basic variables, *cf.* Fig 1.

For the case of a soft and thin elastic layer, this method is motivated by an asymptotic expansion analysis by Klarbring [2]. If the adhesive is flexible enough, the stresses through the thickness are smeared out and the geometrical details at the start of the layer become less important. Thus, the adhesive layer can be described by the relations  $\sigma(w, v)$  and  $\tau(w, v)$ .

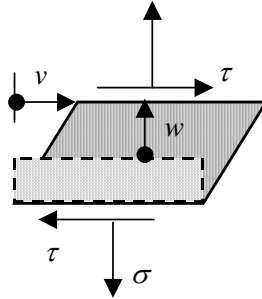


FIGURE 1. Deformation modes of the adhesive layer peel,  $w$ , and shear,  $v$ .

In this paper we only consider peel loading, which can be considered as a special case of the above stated relations. Thus, the  $\sigma$ - $w$  relation is to be determined experimentally. Andersson and Stigh [1] have performed a series of tests on a DCB-specimen, *cf.* Fig. 2. The relation between the peel stress and the elongation for the DCB specimen is given by

$$\sigma(w) = \frac{2}{b} \frac{d(F\theta)}{dw} \quad (1)$$

where,  $F$  is the applied load,  $\theta$  is the rotation of the loading point and  $w$  the elongation of the adhesive layer at the start of the layer. The adherends need to be elastic for eq. (1) to be valid.

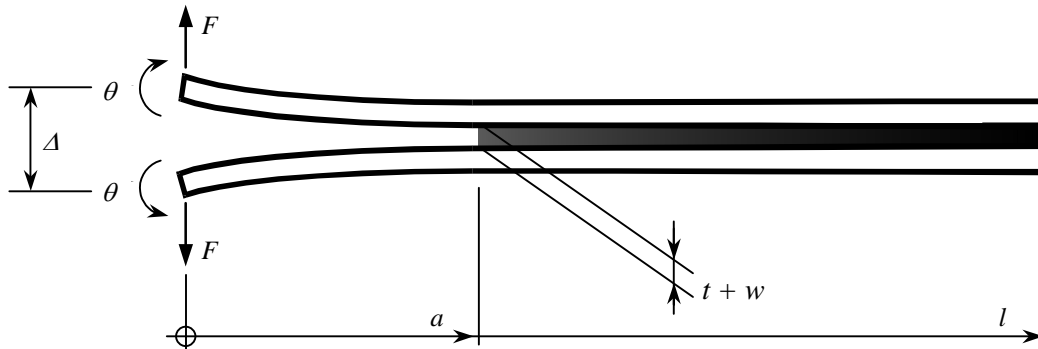


FIGURE 2. DCB-specimen.

A structural adhesive, DOW BETAMATE X-1044, was used in [1] and it was found that the stress-elongation curve could be divided into three parts. First, a linear elastic part, then a part with a constant stress and the curve ends with a parabolically descending part.

The present paper continues the work presented in [1]. In that paper, only slight variations of the geometry of the specimen were studied. Here, we attempt to validate the method by performing experiments on five groups of specimens with different dimensions. By this variation, the length of the damage zone is varied. The extreme case is expected to occur when the adherends undergo extensive plastic deformations. In this case, the length of the damage zone is small and the question is if the measured stress-elongation relation for a large damage zone can be used to predict the behaviour with a short zone.

## 2. Theory

The underlying theory behind eq. (1) is based on the concept of equilibrium of energetic forces as introduced by Eshelby [3]. Here, we merely present the main features of the derivation. For a more comprehensive study, we refer to [1].

The energetic forces acting on the specimen are associated with the positions of the acting loads ( $F$ ) and the start of the adhesive layer. In [2] these energetic forces are derived as

$$J_F = \frac{F\theta}{b}, \quad J_{\text{adhesive}} = \int_0^w \sigma(\tilde{w}) d\tilde{w} \quad (2a,b)$$

where  $b$  is the out-of plane width of the specimen,  $\theta$  is the rotation of the loading point, and  $w$  is the elongation of the adhesive at the start of the layer, *cf.* Fig. 1. Equilibrium of the energetic forces yields

$$\int_0^w \sigma(\tilde{w}) d\tilde{w} = \frac{2F\theta}{b} \quad (3)$$

The number two, on the right hand side of this equation, originates from the fact that two forces ( $F$ ) act on the specimen. Differentiating eq. (3) yields eq (1).

In an experiment the force,  $F$ , the rotation,  $\theta$ , of the loading point and the elongation,  $w$ , is measured simultaneously. The stress-elongation relation is found by either making direct differentiation of measured data or by first using curve fitting and then differentiate the fitted curve. In this paper the latter method is adopted.

A critical requirement for the validity of the method is that the adherends must stay elastic during an experiment. Moreover, if the adhesive layer is unloaded from a non-elastically deformed state, the theory breaks down since the concept of energetic forces no longer work. These two requirements are easily check by use of the finite element method and are avoided in the experiments to determine  $\sigma(w)$ .

## 3. Experimental preparations

### 3.1 Design of specimens for property determination

If the  $\sigma$ - $w$ -curve is a property associated with the adhesive layer, it must be independent of the geometry tested. That is, the curve determined by the use of eq. (1) must be the same for different geometries. A feature that may have a large influence on the relation is the size of the damage zone developing at the start of the adhesive layer during loading. For the DCB-specimen, it can be demonstrated that the height of the adherend has a large effect on the size of the damage zone; stiff adherends leads to large damage zones. Thus, the main emphasis in the present study is set on altering the height of the adherends. All other dimensions are altered only because of the limitations of the tensile test machine that is utilised in the experiments.

By means of a solution in closed form given by Stigh [4] it is possible to evaluate the size of the damage zone approximately. In [4] the stress-elongation relation is described by a saw-tooth shaped curve. Four different groups of specimens were chosen based upon the size of the damage zone. The dimensions of the specimens and the approximate length of the damage zone,  $l_{\text{zone}}$ , are given in Table 1.

TABLE 1. Dimensions (units in mm).

	Group. 1	Group. 2	Group. 3	Group. 4
$b \times h \times L$	5 x 6 x 150	5 x 10 x 200	5 x 16 x 400	5 x 20 x 400
$a$	60	120	200	250
$l_{zone}$	12	17	25	30

The adherends are made of steel with Young's modulus,  $E$  of about 206 GPa. The yield strength,  $\sigma_Y$  is larger than 500 MPa. Note that these data do not enter explicitly in eq. (1). All the specimens are cut to the correct dimensions before gluing. The surfaces of the adherends are cleaned with n-Heptane and are subsequently washed with acetone. After the cleaning, the adhesive is smeared out on one of the adherends and the specimen is clamped together. In this process, Teflon-inserts with a thickness of 0.2 mm are used to achieve the correct adhesive layer thickness. The adhesive is then cured at 180°C for about 30 minutes according to the specification of the manufacturer. The oven is then turned off and the specimen is allowed to slowly cool to room temperature. All the specimens of each Group are placed in the oven at the same time. By this process, we limit possible effects of variations of the manufacturing process.

### 3.2 Experimental setup

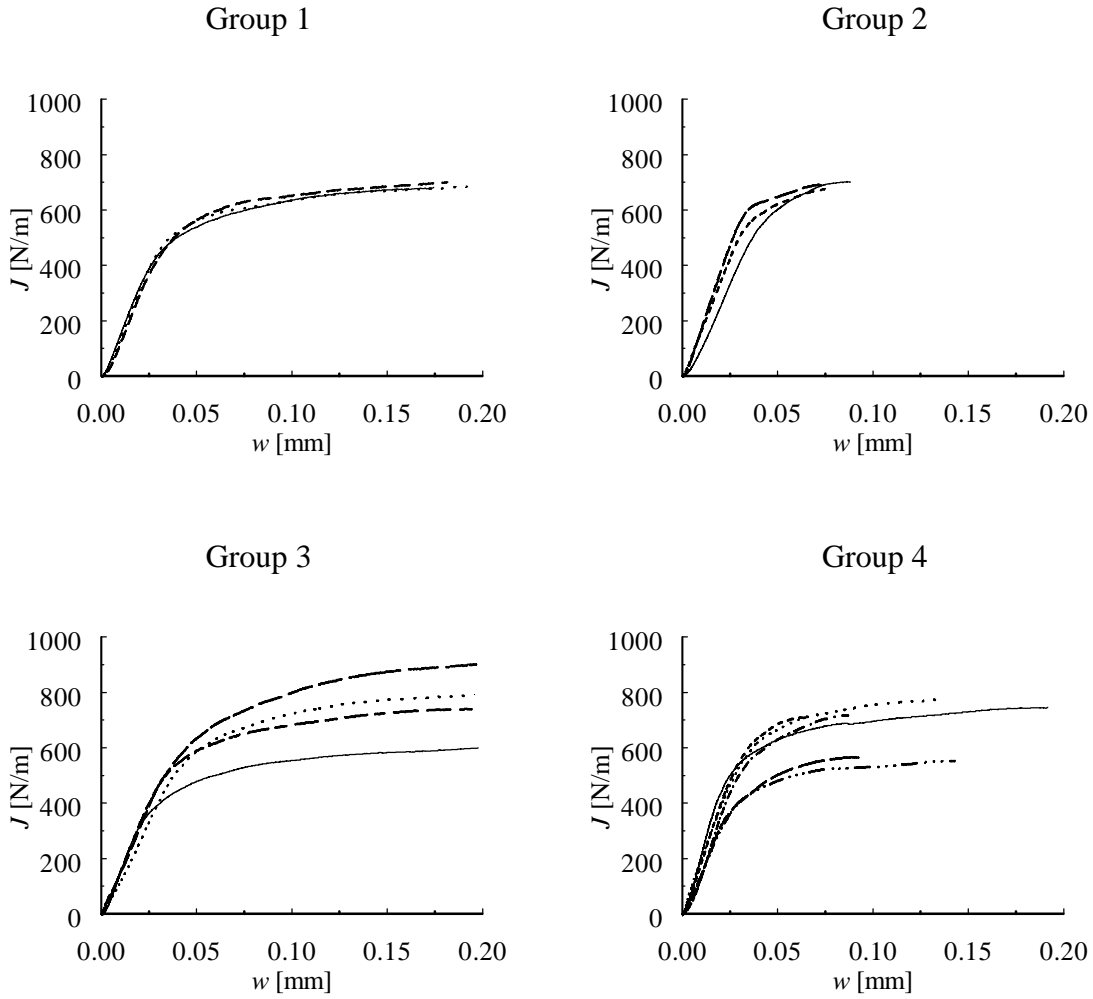
The measurement system consists of a force transducer, a shaft encoder and two LVDT's. The shaft encoder is used to measure the rotation,  $\theta$ , at the loading point and the LVDT's are used to measure the elongation,  $w$ . The LVDT's are placed at the opposite sides of the adherends. Thus, they measure the elongation of the layer, *cf.* Fig. 2.

In [2], the experimental method to measure  $w$  made it impossible to measure the start of macroscopic crack propagation. Therefore, a microscope is utilized in this study to record the deformation at the start of the adhesive layer during the experiment. With the microscope, it is also possible to study the deformation and fracture processes at the start of the layer.

## 4. Determination of the $\sigma - w$ curves

### 4.1 Experimental $J - w$ curves

The experimental  $J - w$  curves are shown in Fig 3. The curves appear smooth and regular indicating that the experiments have been well performed. The curves in Group 1, *i.e.* where the height of the adherends is 5 mm, do almost coincide up to  $w = 0.2$  mm. Visual inspection of the fracture surfaces of the specimens in Group 1 reveals rough surfaces along the entire bond. Group 2 shows similar behaviour as Group 1. However, one curve in Group 2 has a lower initial slope indicating a weaker bond of the layer. Inspection of the fracture surface of this specimen indicates interfacial fracture. This explains the lower slope in this experiment. In Group 3, one experiment particularly distinguishes itself from the others. In this test, the fracture surface contains air bubbles at the start of the layer; this explains the low value of  $J$ . In Group 4 there are two curves that are singled out from the others. One of the specimens shows air bubbles at the start of the layer whereas the fracture surface of the other is considerably smoother than the remaining.

FIGURE 3. Experimental  $J - w$  curve.

#### 4.2 Determination of the $\sigma - w$ curves

The  $\sigma - w$  curve is calculated by first adjusting a curve to the experimental  $J - w$  result. The following series of exponential functions is used

$$J(w) = \sum_{i=1}^n A_i \exp\left(-\frac{nw}{i}\right) \quad (4)$$

The constants,  $A_i$  are determined by means of the least square method. The number of terms  $n$  is varied between 10 to 15. The number finally chosen depends on the experiment. The resulting curves are then differentiated according to eq. (1). The results are shown in Fig. 4. The  $\sigma - w$ -relations agree well within and between the experimental groups. All the experiments show a maximal peel stress of approximately 18 MPa. Slight variations exist in each group. In addition, the  $\sigma - w$  curves are in agreement with the ones found in [2].

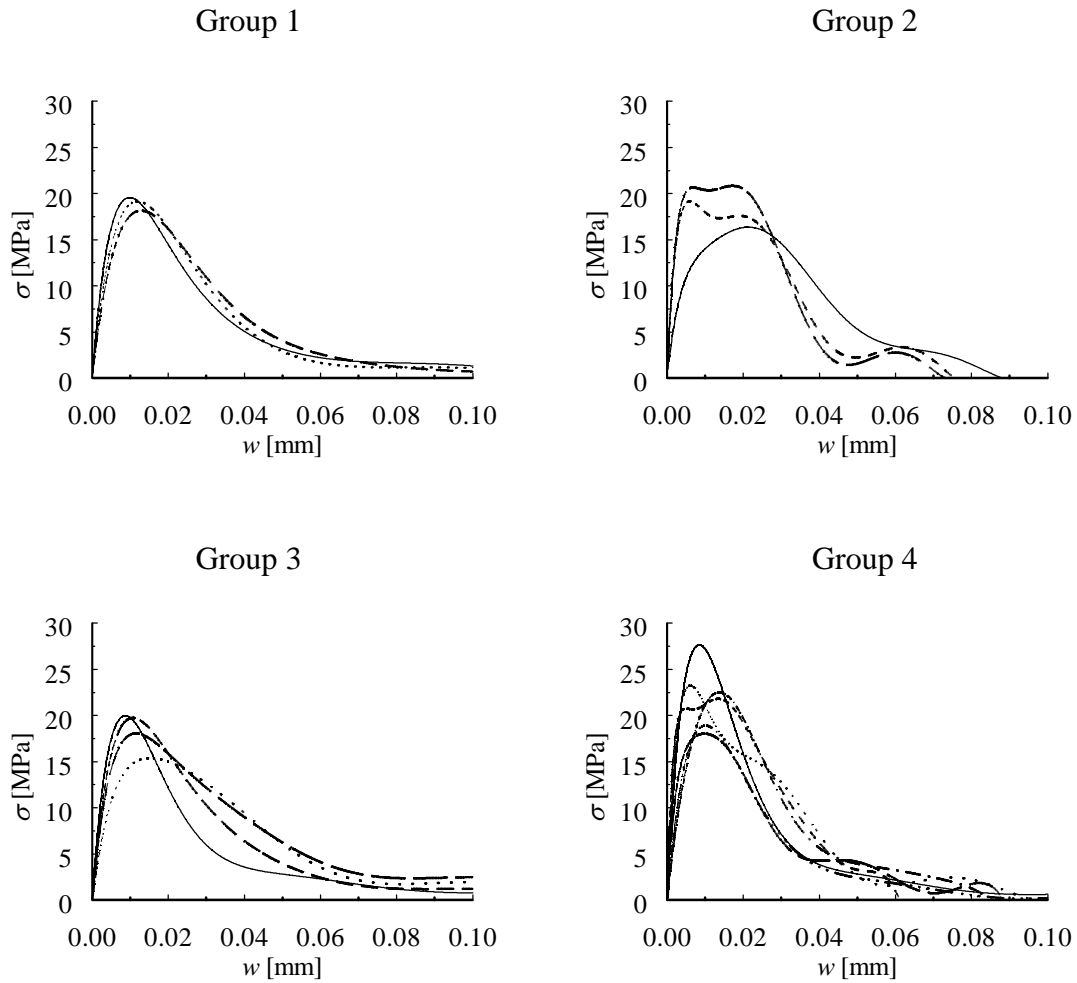


FIGURE 4. Experimental stress-elongation relations.

#### 4.3 Deformation process

The deformation process at the start of the adhesive layer is recorded with a microscope. Figure 5 shows the region at three different states.

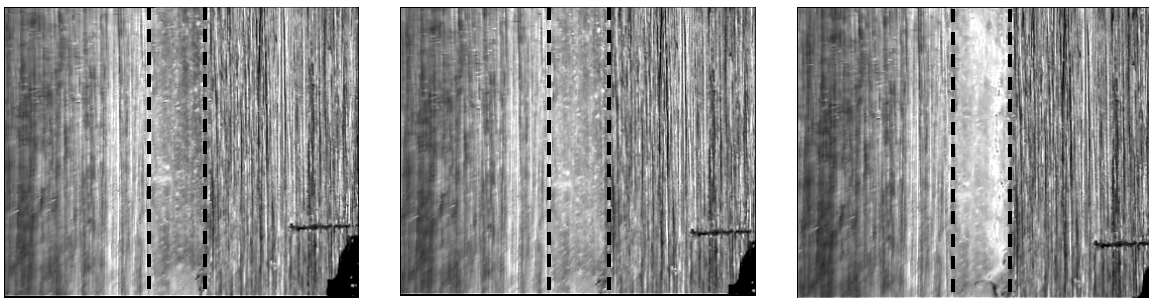


FIGURE 5. Deformation of the adhesive layer. Left: Un-deformed. Middle: At the maximum stress. Corresponding to the square mark in Fig. 6. Right: At the first visible crack. Corresponding to the triangular mark in Fig. 6.

The left photo shows the unloaded layer. At the lower end of this photo, the Teflon insert is visible. The middle photo shows the region at the maximum stress. Some stress whitening is visible at this stage. However, no cracks are visible at this stage. The last photo shows the state when the first cracks are visible. The corresponding points on the  $\sigma$ - $w$ -curve are indicated in Fig. 6.

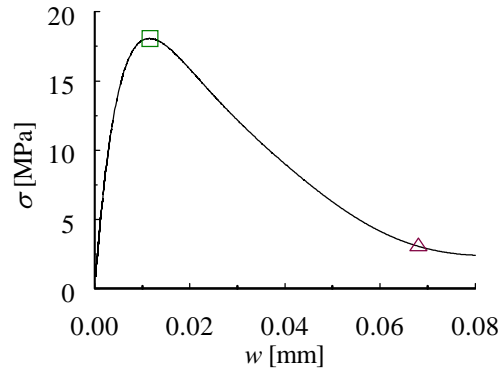


FIGURE 6. Corresponding points on the  $\sigma$ - $w$ -curve.

## 5. Plastically deforming specimens

### 5.1 Design of the plastically deforming specimen

If the adherends are allowed to deform plastically the length of the damage zone can be considerably shortened. In this case, the specimens are designed by means of the finite element method. The commercial program ABAQUS version 5.8 is used for this purpose. The adherends are modelled using beam elements and spring elements are used to model the behaviour of the adhesive layer. The force-displacement curve for the springs follows the stress-elongation relation shown in Fig. 4 (Group 1) where the force is determined according to  $F(w) = \sigma(w)bl_e$  where  $b$  is the width of the adherend and  $l_e$  is the length of the corresponding beam element. In the simulations the critical energy-release rate is set to  $J_c = 700$  N/m.

A mild steel is chosen for the adherends. The material is assumed to be well described by an elastoplastic material model with linear isotropic hardening. In the experiments, the plastic strain never exceeds the limit where the stress-strain curve becomes non-linear. Thus, the assumed linear hardening is accurate enough. In order to determine the parameters of the elastoplastic model, *i.e.* the yield strength,  $\sigma_Y$ , and the hardening modulus,  $H$ , bending tests on the sheet material were performed. By comparing a finite element simulation to the experiments it is found that the experiments can be re-created with  $\sigma_Y = 190$  MPa and  $H = 2.5$  GPa.

With the behaviour of the adherends and the adhesive layer determined as described above, simulations are used to determine an appropriate specimen design. The final design gives a 1 mm thick sheet metal with a total length of 50 mm. The initial crack length is chosen to 25 mm. The width is 6.5 mm. With these values, the adherends are expected to deform plastically before the adhesive loses its loading capacity.

## 5.2 Experimental and numerical results

Three experiments were performed. In the experiments, the adherends first deform plastically, then the adhesive layer starts to fracture and the experiments are finished after about 2 mm crack growth. The results from the experiments and the simulations are shown in Fig. 7. The simulation, considering large deformations, is capable of reproducing the experiments accurately. It is however not clear at present if the results are sensitive to variations in the  $\sigma$ - $w$  curve.

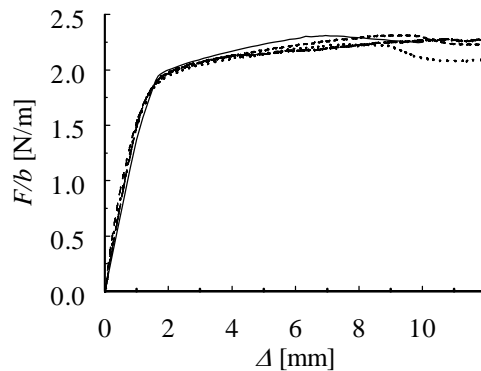


FIGURE 7. Comparison between experiment and simulation for plastically deformed specimen (solid line: simulation, dashed lines: experiment).

## 6. Conclusions

The  $\sigma$ - $w$  relation, found in the experiments, is considered to agree well within and between the experimental groups. Even in the case where the adherends deform plastically, the  $\sigma$ - $w$  relation can be used to predict structural behaviour. This supports that the  $\sigma$ - $w$  relation can be used as a material law for the adhesive layer. The experiments performed in this paper indicate that the length of the damage zone is of minor importance. However, slight differences exist in the experiments. Group 3 shows a larger scatter in the  $J$ -curves as compared to the other groups. However, no apparent difference in the fracture surfaces can be observed between the specimens in this group. In Group 4, the maximum peel stress varies between 18-27 MPa. In this group, the crack has a tendency to jump between the interfaces rather than propagating in the adhesive. Moreover, the fracture surfaces of Group 4 contain regions where the surface is almost smooth. These regions appear randomly distributed over the surface.

## References

1. Andersson, T., and Stigh, U., *International Journal of Solids and Structures*, vol. **41**, 413-434, 2004
2. Klarbring, A., *International Journal of Engineering Science*, vol. **29** (4), 493-512, 1991
3. Eshelby, J. D., *Philosophical Transactions of the Royal Society of London Series A* **244**, 87-112, 1951
4. Stigh, U., *International Journal of Fracture*, vol **37**, R13-R18, 1988